

# Optical Engineering

OpticalEngineering.SPIEDigitalLibrary.org

## **Optical fiber ring resonator as a high-resolution spectrometer. Characterization and applications with single line diode lasers**

Damian Presti  
Fabian A. Videla  
Gustavo A. Torchia

**SPIE.**

Damian Presti, Fabian A. Videla, Gustavo A. Torchia, "Optical fiber ring resonator as a high-resolution spectrometer. Characterization and applications with single line diode lasers," *Opt. Eng.* **57**(5), 057108 (2018), doi: 10.1117/1.OE.57.5.057108.

# Optical fiber ring resonator as a high-resolution spectrometer. Characterization and applications with single line diode lasers

Damian Presti,<sup>a,b</sup> Fabian A. Videla,<sup>a,b</sup> and Gustavo A. Torchia<sup>a,b,\*</sup>

<sup>a</sup>Centro de Investigaciones Ópticas CONICET La Plata-CICBA-UNLP, M.B. Gonnet, Buenos Aires, Argentina

<sup>b</sup>Universidad Nacional de Quilmes, Departamento de Ciencia y Tecnología, Buenos Aires, Argentina

<sup>c</sup>Universidad Nacional de La Plata, Departamento de Ciencias Básicas, Facultad de Ingeniería, Buenos Aires, Argentina

**Abstract.** An optical fiber ring resonator (OFRR), a wavelength sensor for testing a single-mode laser system in a wide range of temperature, is presented. We will show that it is possible to calibrate, in relative form, a scale of wavelength, to determine, accurately enough, a thermally induced laser detuning, using the free spectral range of an OFRR. The optical circuit was constructed using  $2 \times 2$  (50/50) optical fiber coupler obtaining an OFRR of 10-cm ring radius. A single-mode diode laser system has been launched into the OFRR, and different experiments have been performed. We tested the OFRR performance, considering fluctuations in the laser wavelength caused by small temperature instabilities, measuring the output intensity from the ring resonator. Theoretical simulations and experimental results were in agreement with the expected behavior. Furthermore, OFRR systems can be used as an excellent control tool to test the wavelength stability for a narrowband laser diode and act as a part of a control system. © 2018 Society of Photo-Optical Instrumentation Engineers (SPIE) [DOI: [10.1117/1.OE.57.5.057108](https://doi.org/10.1117/1.OE.57.5.057108)]

Keywords: fiber optics; ring resonator; single-mode lasers; temperature control system.

Paper 171908 received Nov. 29, 2017; accepted for publication May 9, 2018; published online May 24, 2018.

## 1 Introduction

During the last few decades, optical sensors have been successfully used in many fields of application to study the performance of several physical magnitudes. Among these optical devices, nowadays, optical ring resonator (ORR) systems are involved in very up-to-date research topics on several fields of application, such as sensors with different purposes for instance temperature,<sup>1</sup> angular velocity,<sup>2</sup> stress,<sup>3</sup> pressure, etc., as well as optical elements for integrated optics in optical communication (WDM,<sup>4,5</sup> filters, lasers,<sup>6</sup> Bragg gratings),<sup>7</sup> and chemical and health monitoring,<sup>8,9</sup> among others.

Optical sensors present several advantages with respect to other systems; in particular, optical sensors can be operated independently of variations in different external parameters, such as temperature, vibration, electromagnetic noise, etc.<sup>10-14</sup> This means that external fluctuations can be easily decoupled from the main sensed signal. These sensors work using reference signals to control the outside variations. This last technique is explained in depth in reference.<sup>11</sup>

On the other hand, laser systems are generally designed and used to interrogate these optical sensors; in this way, narrowband laser, high-resolution spectrometers, and high signal/noise ratio detectors are necessary to accurately and reliably measure the physical properties tested. Distributed feedback (DFB) lasers are an example of narrowband laser whose fluctuations in wavelength and intensity have been studied and characterized. The typical DFB laser is based on a single-mode semiconductor structure (based

on a Bragg grating) when operating in the range of 0°C to 70°C. It has a tunability of 0.1 to 0.2 nm/°C.<sup>15</sup> This type of laser is always associated with a thermistor-based probe that operates by measuring the temperature at the level of the semiconductor encapsulation and a thermo-electric cooler (TEC) modulus driven by a current that must take values such as to stabilize the temperature of the case.<sup>16</sup>

Thermal stability of the narrow laser sources is a key point when they are used to interrogate ring resonators-based devices; it will be shown that the transfer function (TF) of this device is sensitive enough to detect changes in wavelength. In this sense, the temperature effects on the optical fiber ring resonator (OFRR) and DFB laser responses must be known to design and evaluate the OFRR as a device able to produce a reliable wavelength interval. To start the analysis, we first consider an example to fix ideas of ranges commonly used.

Fixing at 15°C, the encapsulation while the room temperature changes from 15°C to 35°C, Asmari et al.<sup>15</sup> reported a wavelength drift rate of  $-3.8 \pm 0.5$  pm/°C. In that paper, it was proposed to improve the reduction of the aforementioned rate to 0.03 pm/°C, by measuring the junction voltage of the semiconductor diode, considering the relationship between voltage, current, and junction temperature, avoiding measuring case temperature.

In our work, we show that when the DFB device operates within the temperature range of 30°C to 70°C and the temperature control attached to DFB device is on, the wavelength shift (detuning) due to an increase in the external temperature is appreciable lower than those reported in the range of 15°C to 35°C. The heat sink attached to our DFB device is sufficient to evacuate the heat introduced by the environment.

\*Address all correspondence to: Gustavo A. Torchia, E-mail: [gustavot@ciop.unlp.edu.ar](mailto:gustavot@ciop.unlp.edu.ar)

In this paper, we show that an OFRR can be used as an optical sensor to test a single-mode laser system by measuring the wavelength detuning originated when the device is tested between 30°C and 70°C. The DFB detuning is evaluated considering the free spectral range (FSR) of the OFRR as a “unit” of the wavelength scale. These characteristics and behavior of the OFRR + DFB system can be summarized to explore departures on wavelength versus temperature and also to evaluate limits within the useful temperature range.

## 2 Materials and Methods

### 2.1 Ring Resonator

As it is well known, the basic physical concept supporting the ORR systems relies on the Fabry–Perot resonator.<sup>17</sup> Considering a simple configuration, the ORR works with only one input/output waveguide whose optical radiation is coupled or decoupled to the ring resonator at regular wavelength intervals as indicated in Fig. 1(a).

In these systems, many resonances satisfying Fabry–Perot conditions can be easily detected at the output, and they follow the TF expression given by<sup>18</sup>

$$TF(\omega) = \frac{(\sigma - \tau)^2 + 4\sigma\tau \sin^2\left(\frac{\omega LN}{2c}\right)}{(1 - \sigma\tau)^2 + 4\sigma\tau \sin^2\left(\frac{\omega LN}{2c}\right)}, \quad (1)$$

where  $\tau$  is a coupling coefficient between the ring and the output,  $\sigma$  is the total guide loss coefficient (associated with electromagnetic fields),  $L = 2\pi R$  is the traveled distance inside the resonator (ring perimeter),  $N$  is the effective guiding index, and  $\omega$  corresponds to the propagated light frequency.

Other important characteristic for the OFRR is the FSR. This parameter is defined as the frequency interval between each dip from the TF and follows the expression given by

$$\Delta\lambda_{FSR} = \frac{\lambda^2}{LN}. \quad (2)$$

By taking into account the dimensions of the ring, the TF, which represents the ORR sensitivity, is similar to that shown in Fig. 1(b) (blue solid line). Curve parameters were set by considering the low propagation losses for the optical fibers (<0.1 dB/km). Also taking into account a spectral narrow-band source that is able to sweep a spectral range (red solid line) to produce the optical response, the output intensity was calculated as function of the frequency for the coupled light. The ORR, presented in this work, consists of a 10-cm ring radius, whose FSR is 2.58 pm, corresponding to 800 MHz at  $\sim 1.55 \mu\text{m}$ . By calculating the total derivative of Eq. (2), the effect of wavelength, refractive index, and radius uncertainties on FSR wavelength peaks position can be evaluated

$$\Delta FSR = \frac{\Delta N1 \left| \frac{\lambda^2}{N1^2 R} \right|}{2\pi} + \frac{\Delta R \left| \frac{\lambda^2}{N1 R^2} \right|}{2\pi} + \frac{\Delta \lambda1 \left| \frac{\lambda}{N1 R} \right|}{\pi}. \quad (3)$$

After calculations, considering  $\lambda = 1.55 \times 10^{-6}$  m,  $N1 = 1.45$ ,  $R = 0.1$  m and the estimated uncertainties in the measurements of wavelength, refractive index and the ring radius as  $\Delta\lambda1 = 10^{-10}$ ,  $\Delta N1 = 10^{-3}$   $\wedge$   $\Delta R = 0.015$ , respectively, we have obtained  $\Delta FSR = 3.5 \times 10^{-13}$  m. It is worth mentioning that the main contribution to Eq. (3) is given by the third term despite the fact that its multiplier is lower than the first one, as it follows:

$$\begin{aligned} \frac{\lambda}{N1 R \pi} &= 3.1 \times 10^{-6}, & \frac{\lambda^2}{N1^2 R 2\pi} &= 1.6 \times 10^{-12}, \\ \frac{\lambda^2}{N1 R^2 2\pi} &= 2.3 \times 10^{-11}. \end{aligned} \quad (4)$$

### 2.2 Transfer Function of an OFRR. Temperature Response of the OFRR

An important point to consider is related to the changes in the external temperature surrounding to the OFRR. For this reason, at first, it should be necessary to consider a modified optical response (TF). In this sense, the changes of temperature effects modify two important parameters on the OFRR; one of these is the length of the ring (dilatation or contraction) as well as the refractive index of the optical fiber. However, these changes could be neglected in the TF due to its slow rate of fluctuations compared to those occurring in the laser.

### 2.3 DFB Diode Laser System. Effects of Temperature Variation

Effects of temperature variation on the laser diode system must be considered. Among others, three main parameters are temperature sensitive in these devices: output power, working wavelength, and finite spectral width. From the above-mentioned three parameters, we are concerned with wavelength. Wavelength shift is caused by the thermal expansion in the Bragg grating period whose expansion coefficient is 0.014 nm/°C for a typical laser, being its effective refractive index of 3.6.<sup>19</sup> Refractive index is, in turn, temperature sensitive. Grating can absorb heat coming from the external environment and alternatively from the injection

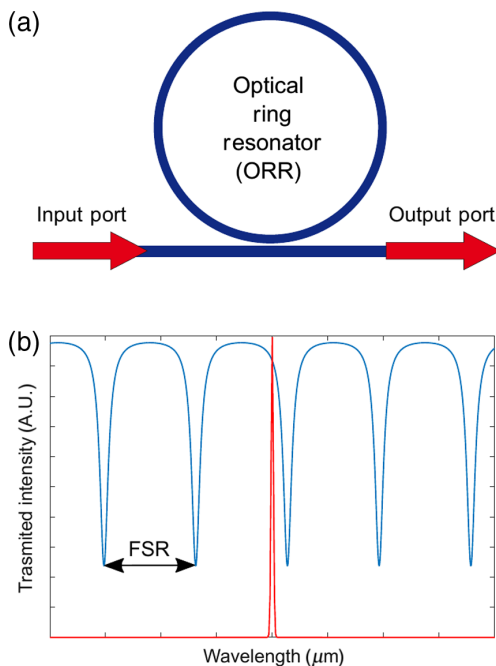


**Fig. 1** (a) ORR schematic and (b) TF ( $\lambda$ ) or transmittance of ring resonator. The red line represents the narrow laser (width not at scale) used to interrogate the OFRR system. The FSR is also indicated by arrows in this figure.

current as a result of the Joule effect. Experimentally, in Ref. 19, it was shown that the laser temperature and the injection current have a linear relationship from  $0.006^{\circ}\text{C}/\text{mA}$ , and the effect on wavelength was evaluated in  $0.374\text{ GHz}/\text{mA}$  ( $3.3\text{ pm}/\text{mA}$ ).<sup>16</sup> Despite those effects, environment heat contribution produces the main wavelength detuning because of the temperature response of the diode, fact registered during the interrogation process on the OFRR. Without action of the temperature control, the wavelength variation versus the temperature, characteristic given by the manufacturer ( $0.2\text{ nm}/^{\circ}\text{C}$ , QPhotonics Inc.), could be detected by observation. The TF for the OFRR as a function of wavelength detuning is detailed in Fig. 2.

Another important feature of DFB lasers is their finite spectral width. This is mainly due to spontaneous emission whose phase is random and is coupled to the laser mode. Instead of a discrete energy transfer as in the gaseous laser, the semiconductor lasers are characterized by a gain spectrum several times wider than the longitudinal mode spacing. Consequently, fluctuation in gain increases the spectral line width. However, in Fig. 2, this broadening cannot be appreciated in the representation of the OFRR spectrum because frequencies scale of our experiments.

To explain the fluctuating aspect of the TF measurements, we have modeled this effect as a convolution between the laser and the ring resonator spectrum. Under not stabilized environmental conditions and regarding the effects stated above, it is convenient to introduce a third option to describe the TF for the OFRR. In particular, the actual temperature behavior of the laser diode junction is sensitive to temperature fluctuation around the working point (i.e.,  $25^{\circ}\text{C}$ ), with a whole amplitude range of  $0.1^{\circ}\text{C}$ , taking into account the action of the temperature control system associated to the laser. To show in detail, this variation in the surrounding of a resonance peak, we have considered a fluctuation temperature interval of  $0.01^{\circ}\text{C}$ . Convolution between the TF and laser wavelength spectrum can be shown in Fig. 3. As it can be seen, small temperature variations in the laser diode cause a wavelength detuning; they were described by an oscillating function (sine) with temperature. This picture describes in an illustrative way the effect of temperature variation on the laser diode junction, so adding a certain

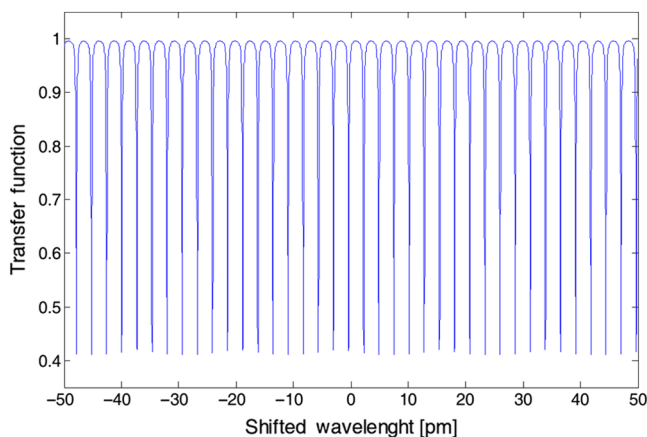


**Fig. 2** Simulated TF response of the laser coupled to the OFRR considering a drift rate of  $0.2\text{ nm}/^{\circ}\text{C}$ . The overall temperature change was set to  $0.5^{\circ}\text{C}$ .

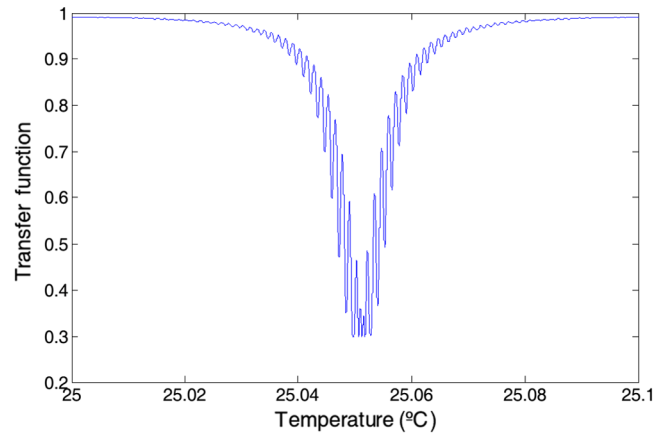


**Fig. 3** Simulated optical response for the OFRR considering an oscillating wavelength detuning of  $0.01^{\circ}\text{C}$ . This illustrates the optical response to slight temperature changes in the OFRR sensor when the temperature laser controller is active.

degree of wavelength detuning at the output results in a more realistic visualization of the OFRR response.

## 2.4 Experimental Procedure

In this work, the OFRR used to test a single-mode laser system was constructed using a  $2 \times 2$  50/50 fiber coupler (Newport F-CPL-F22155), as sketched in Fig. 4. The OFRR was designed with a 10-cm radius and with fiber channel/angle physical contact connectors at the input and output to connect the analyzed laser and the photodiode detector, respectively.

Single-mode laser system was used to analyze the operation of the optical fiber device. The laser and its associated control were manufactured by QPhotonics. The laser has a wavelength detuning with temperatures of  $0.2^{\circ}\text{C}/\text{nm}$  (without control), 10-mW output power, and 2-MHz bandwidth ( $0.01\text{ pm}$ ).

The detection system is composed of three main parts. The first of these converts the optical output power from the OFRR into an electric current. To do that, a photodiode (FGA04 InGaAs) with a fast response and high signal/noise ratio is used. After that, the current is converted into a voltage to amplify the signal using a transimpedance amplifier (second stage). Finally, in the third stage, a microcontroller handles the sampling and then transmits the data to the PC.

As it was stated above, to test the optical response at the system output, the above laser was launched at the OFRR system. Additionally, to clarify the experimental procedure

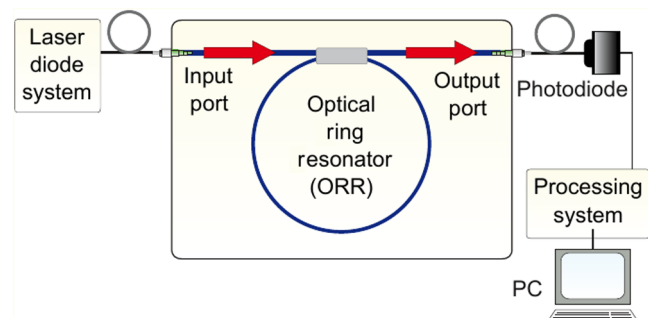


**Fig. 4** Block diagram for the sensing system used in this paper.

used to carry out the experiments presented in this paper, a block diagram has been presented in Fig. 4.

### 3 Experimental Results and Discussion

To demonstrate the suitable operation of the OFRR and to analyze the performance of the single-mode laser system tested in this work, several experiments were conducted.

First of all, we consider an analytical calculation from Eq. (1) corresponding to wavelength shift between each deep in the TF. In this way, we can calculate the ring resonator TF and then discuss properly the data obtained experimentally. Also by considering Eq. (2), a ring radius of 10 cm and  $N \approx 1.45$  for  $\lambda \approx 1.5476 \mu\text{m}$ , we have calculated an FSR  $\approx 2.58 \text{ pm}$ .

In contrast to the previous predictions, the experiment carried out consisted in performing a forced wavelength detuning in the laser system used and then measuring this effect using the OFRR. This provides the necessary information to perform a detailed analysis of the laser system wavelength shift in function of the environment operating temperature.

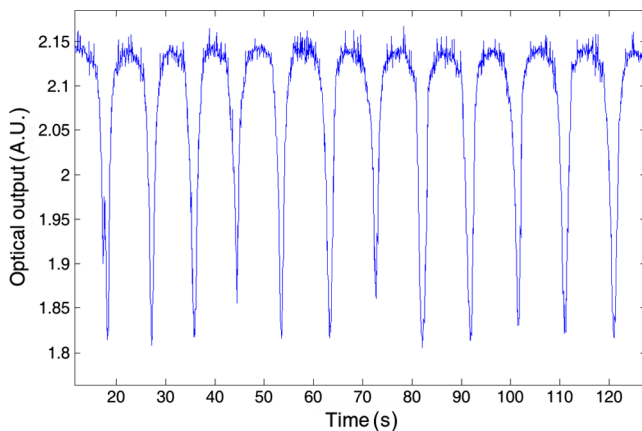


**Fig. 5** Experimental data from the OFRR when a diode laser undergoes a wavelength detuning due to an external forced temperature change when it is working without temperature control.

To do this, we modify the environment operating temperature by means of an external heat source near the laser system setup. Temperature increment produces a monotonically shift in the laser wavelength.

In a first step, we need to turn off the internal temperature control loop of the laser controller. In this way, we leaved the laser diode system free (self-riden) to respond to the external temperature disturbances. Measuring these effects is supported by the filtering action of the OFRR.<sup>20</sup> Under the above-mentioned conditions, the optical response as a function of time, which is represented in Fig. 5, was obtained.

As it can be seen, several resonances took place. Large dips appear at regular periods of time, showing that wavelength detuning caused by the heat exchange between the laser system and the surrounding medium is a process slowly developed. In this sense, the wavelength detuning gives rise to a typical optical response from the OFRR as is shown in Fig. 2.

Figure 6 represented the theoretical TF from Eq. (1), for the first seven dips and additionally the experimental values measured. All values have been normalized to better perform the comparison. These data were taken at the beginning of the heating process, that is, when the heat source was applied to the DFB diode to produce their shifting in wavelength. The temperature interval corresponding to the seven represented peaks based on Fig. 2 was of  $0.066^\circ\text{C}$ . The experimental peaks are in good agreement with the theoretical ones; this fact enables to determine some characteristic parameters of the OFRR, such as FSR, attenuation, losses, coupling coefficient, and finesse. FSR was evaluated as a mean value of several wavelength intervals among peaks. Finesse was evaluated considering FSR divided by the full width at half maximum (FWHM). As it can be seen, resolutions in abscissa axis are in the order of picometers. Table 1 summarized the values of resonances and simulation parameters.

In a second step, the test on the OFRR is repeated, but in this case with the temperature control loop on. From this experimental data, shown in Fig. 7(a), again the resonances can be attributed to the OFRR TF response when a laser diode undergoes a wavelength detuning that can shift

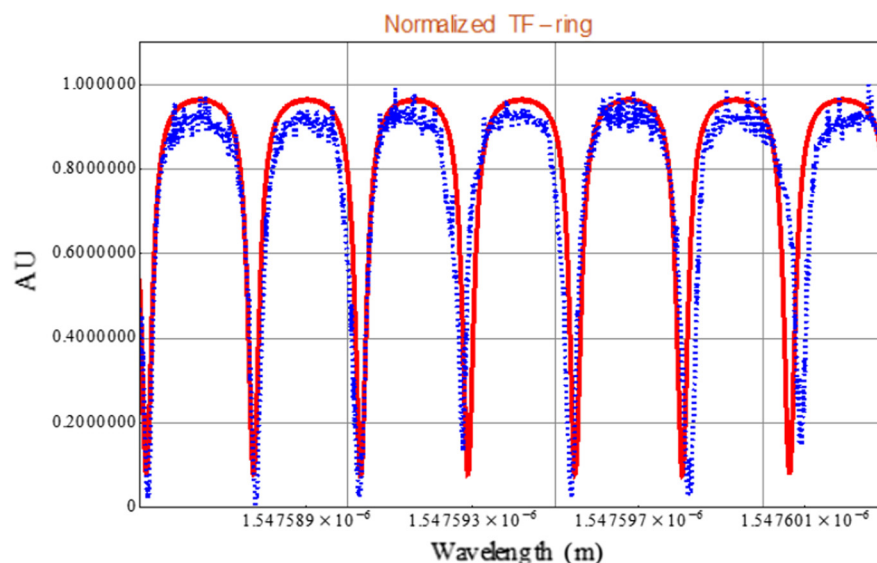


**Fig. 6** Normalized experimental data (blue dots) from the OFRR excited by a DFB laser under a temperature variation and simulated values (red solid line) from Eq. (1).

**Table 1** Calculated values for FSR finesse and attenuation show good agreement with the experimental ones, despite of low finesse calibration in wavelength allows to obtain enough accuracy to determine the degree of detuning of a DFB laser.

	FT fit (m)	Ring parameters
FWHM	$2.9971 \times 10^{-13}$	—
Peak	$1.54758517 \times 10^{-6}$	—
Peak	$1.54758774 \times 10^{-6}$	—
Peak	$1.54759032 \times 10^{-6}$	—
Peak	$1.54759290 \times 10^{-6}$	—
Peak	$1.54759548 \times 10^{-6}$	—
Peak	$1.54759805 \times 10^{-6}$	—
FSR	$2.58 \times 10^{-12}$	—
Finesse	8.6	—
Radius	—	0.102
Attenuation $\alpha$ (cm <sup>-1</sup> )	—	0.4
Loss $\sigma$	—	0.774
Coupling $\tau$	—	0.866

along a dip interval, that is, around of the resonance corresponding to the OFRR system designed in our experiments. Near from resonance values, it is easy to see a rippled structure that in first approximation can be associated with the optical noise originated in different sources: the detector, laser power, external vibration, etc. However, when each of these resonances is more deeply inspected, it is found that narrow dips are randomly occurring. These fluctuations are due to rapid changes in laser wavelength induced by the laser diode controller because of the time response of the system to stabilize the diode junction temperature (see the inset in this figure). This last result could be glimpsed from the simulation in Fig. 3. To show the correlation between the resonance peaks with temperature, we make Fig. 7(a). Additionally, in Fig. 7(b), the evolution of the external temperature change versus time is presented.

Taking into account the parameters of the ring and the optical response shown in Fig. 2, many resonances can be expected. The experimental values obtained in Fig. 7 are in agreement with the theoretical predictions stated above (shown in Fig. 3). We can assume that the calculated value for the FSR through Eq. (4) is the same to that obtained experimentally from Figs. 5 and 6. This means that we can correlate the time axis with the wavelength detuning axis. In this way, the number of dips that we see in Figs. 5 and 6 will be proportional to the laser output wavelength shift. In the case of Fig. 7, in ~30 min (~2000 s), there are five dips in the OFRR output. Therefore, it is equivalent to a distance in wavelength shift of four times FSR. Doing the same in several points of the figure, we can retrieve a graph corresponding to the system wavelength shift as a function of the external temperature as it is shown in Fig. 8. We have considered the initial stabilized wavelength value at initial

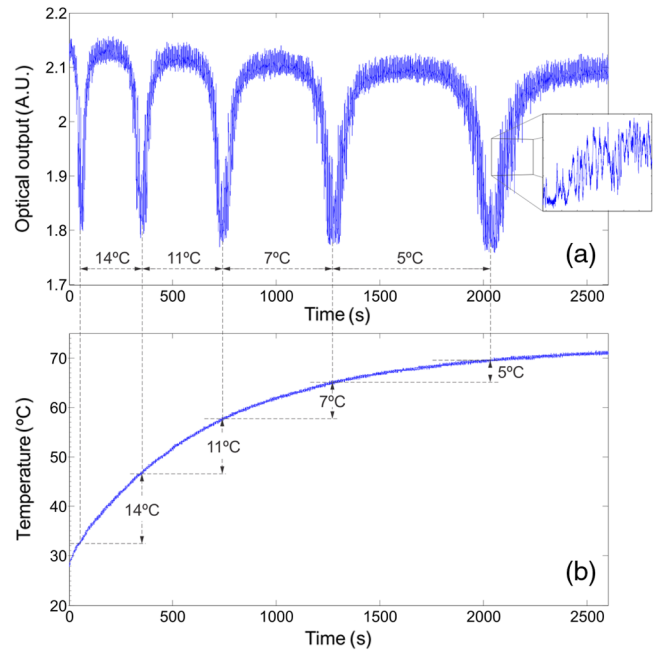


**Fig. 7** Experimental data from the OFRR when a diode laser undergoes a wavelength detuning because of external forced temperature changes with the control loop set on: (a) optical response and (b) evolution of the external temperature. Inset shows the output fluctuations explained in Sec. 3.2.2.

time in agreement with the manufacturer data sheet specified under typical experimental conditions, this value is 1547.6 nm. It is worth mentioning that measured values of wavelength are in the order of commercial ones, such as the wavelength meter (Agilent AG86122B) with a precision of  $\pm 0.15$  pm and an absolute accuracy of  $\pm 0.3$  pm. In our system, FSR is about 2.6 pm, and changes can be solved with resolution closest to commercial equipment. In the last part of Sec. 3.1, calculations have yielded an uncertainty of 0.35 pm. This value is an acceptable uncertainty for our measure of five times FSR, that is, ~13 pm. This curve allows establishing a correspondence between wavelength and temperature. For this curve, it is possible to consider two

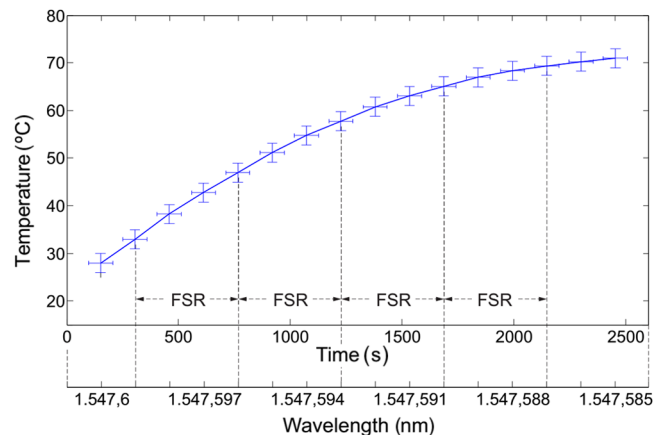


**Fig. 8** Laser system wavelength variation with temperature. For sake of clarity, time and wavelength scales are represented having opposite directions.

ranges between 30°C and 55°C, where uncertainty bars for temperature slightly overlapped, and another between 55°C and 65°C, where they reach a full overlapping.

It is noticed how the slope for curve changes as the temperature increases. In turn, this fact contrasts with some reports given in other works, where similar TEC Thermistor DFB system is used<sup>15</sup> showing linear relationships between temperature and controlled wavelength. Also, it can be observed that wavelength span is about 15 pm in the range of 30°C to 70°C temperature environmental change.

The uncertainty in each point in wavelength is mainly determined by calculation of the FSR of the fiber ring [see Eq. (2)]. The uncertainty in temperature is given for the uncertainty in the thermocouple system  $\pm 2^\circ\text{C}$ . This is directly associated with the action of the temperature controller, it means, the thermoelectric cooler tries to set it at its nominal temperature. When the temperature difference between the environment and case is lower than a minimum limit, the thermoelectric cooler is unable to cool appropriately the diode junction and then wavelength shift curve strongly changes the dependence with temperature. In this way, the temperature control for the laser system only keeps its maximum constant value. Finally, Fig. 8 shows the entire wavelength shift range of a diode laser system under different operation temperatures tested in our work. The FSR associated to temperature increment is indicated in this figure in agreement to Fig. 6.

#### 4 Conclusions

In this paper, we present an OFRR made by assembling commercial  $2 \times 2$  (50/50) optical fiber coupler. Using this optical device, single-mode laser system behavior has been explored in a broader range of environment temperatures. To achieve this, we have forced the laser to operate sweeping a range of environmental temperatures between 30°C and 70°C.

When the temperature control is on, the thermal derive of the laser as a source wavelength is obviously different from those given by the manufacturer. From the analysis of measured data, we have found the actual response for the working point as a function of the external temperature and the range where wavelength fluctuations of the system occur.

It is remarkable that the accuracy to measure small wavelength shifts using a fiber ring, especially when the control is on and these fluctuations are relatively small. Estimated FSR of an OFRR has showed enough accuracy to calibrate the wavelength scale and determine shifts that undergo the laser system when the environmental temperature changes. In addition through the analysis of the presented results, it is possible to establish the correct strategy to design the software/hardware control for the laser wavelength detuning if more accuracy in temperature control was necessary considering the response found in this work. Finally, we can conclude that the OFRR presented in this work can be a powerful tool for testing the performance of single-mode diode lasers if we are focused in the wavelength shift. The procedures followed here can be useful for characterizing the stability operation in similar systems under different boundary conditions (temperature fluctuations) and working points in agreement with the selected mean temperature.

Using this kind of optical sensor, it is possible to ensure high wavelength accuracy when measuring single-mode

lasers, as in the case when highly monochromatic laser sources are required. For example, when this type of laser sources is used for optical communications, we can determine the wavelength bandwidth limit for each channel for designing high data transmission optical path.

#### Acknowledgments

This work was partially supported by the Agencia Nacional de Promoción Científica and Tecnológica, Argentina, under the Project No. PICT-2016-4086. F.A.V. belongs to the Comisión de Investigaciones Científicas, Buenos Aires, Argentina. G.A.T. and D.P. are with CONICET, Argentina.

#### References

1. J. Li et al., "A high sensitivity temperature sensor based on packaged microfiber knot resonator," *Sens. Actuators, A* **263**, 369–372 (2017).
2. Z. Xie et al., "Resonance characteristics of fiber optic ring resonator in fiber optical resonator gyroscope," *Proc. SPIE* **3552**, 267–271 (1998).
3. Y. Yang et al., "Fiber loop ring down for static ice pressure detection," *Opt. Fiber Technol.* **36**, 312–316 (2017).
4. Q. Xu et al., "WDM silicon modulators based on micro-ring resonators," in *19th Annual Meeting of the IEEE Lasers and Electro-Optics Society (LEOS '06)*, pp. 647–648 (2006).
5. J. Muller et al., "High speed WDM interconnect using silicon photonics ring modulators and mode-locked laser," in *European Conf. on Optical Communication (ECOC '15)* (2015).
6. H. Tsuchida, "Limitation and improvement in the performance of recirculating delayed self-heterodyne method for high-resolution laser lineshape measurement," *Opt. Express* **20**, 11679–11687 (2012).
7. A. Othonos and K. Kalli, *Fiber Bragg Gratings: Fundamentals and Applications in Telecommunications and Sensing*, Artech House, Massachusetts (1999).
8. S. Zheng, "Long-period fiber grating moisture sensor with nano-structured coatings for structural health monitoring," *Struct. Health Monit.* **14**(2), 148–157 (2014).
9. S. Zheng, M. Ghandehari, and J. Ou, "Photonic crystal fiber long-period grating absorption gas sensor based on a tunable erbium-doped fiber ring laser," *Sens. Actuators, B* **223**, 324–332 (2016).
10. A. M. Gutierrez et al., "Ring-assisted Mach-Zehnder interferometer silicon modulator for enhanced performance," *J. Lightwave Technol.* **30**, 9–14 (2012).
11. D. G. Rabus, *Integrated Ring Resonator: The Compendium*, Springer-Verlag, New York (2007).
12. K. Suzuki, K. Takiguchi, and K. Hotate, "Monolithically integrated resonator microoptic gyro on silica planar lightwave circuit," *J. Lightwave Technol.* **18**, 66–72 (2000).
13. A. Melloni and M. Martinelli, "Synthesis of direct-coupled-resonators bandpass filters for WDM systems," *J. Lightwave Technol.* **20**, 296–303 (2002).
14. M. Terrel, M. J. F. Digonnet, and S. Fan, "Performance comparison of slowlight coupled-resonator optical gyroscopes," *Laser Photonics Rev.* **3**, 452–465 (2009).
15. A. Asmari et al., "Wavelength stabilisation of a DFB laser diode using measurement of junction voltage," *Proc. SPIE* **9135**, 91351A (2014).
16. H. Ghafouri-Shiraz, *Distributed Feedback Laser Diodes and Optical Tunable Filters*, John Wiley & Sons, Ltd., Chichester (2003).
17. J. P. Chambers, "High frequency Pound-Drever-Hall optical ring resonator sensing," Doctoral Dissertation, Texas A & M University (2007).
18. P. Yeh and A. Yariv, *Photonics: Optical Electronics in Modern Communications*, Oxford University Press, New York (2007).
19. N. Yulianto et al., "Tunability technique of microwave frequency generator using temperature controller and injection current effect of DFB laser," in *AIP Conf. Proc.* (2016).
20. D. A. Presti, F. Videla, and G. A. Torchia, "Design, development and characterization of a DFB (distributed feedback) laser diode control system," in *XVI Workshop on Information Processing and Control (RPIC)* (2016).

**Damian Presti** graduated as an automation and industrial control engineer from Universidad de Quilmes, Argentina, in 2015, where he also works as a professor since 2017. Currently, he is pursuing his PhD funded by CONICET at Centro de Investigaciones Ópticas, La Plata, Argentina. His main research area is integrated optical circuits, in particular focusing on the study of electro-optic modulators made by femtosecond laser writing technique.

**Fabian A. Videla** received his PhD in 2011. Since 1991, he is a professor at Universidad Nacional de La Plata and develops his research at the Centro de Investigaciones Opticas. From 1998, he is a member of the Scientific Research Commission of Buenos Aires Province. He is the author of about 40 scientific articles, including particle sizing and light scattering, air pollutant measurements, nanoparticles field enhancement, photonics circuits, and research in engineering teaching. He is a member of SPIE and OSA Student Chapters.

**Gustavo A. Torchia** received his PhD in physics from Universidad Nacional de La Plata, Argentina, in 2000. From 2005, he is a member of the National Research Council of Argentina. He is author of more than 80 scientific articles. His main research areas are ultrashort laser writing, luminescence and Raman confocal spectroscopy, and development of integrated optical devices. He also is a professor at Universidad Nacional de Quilmes and an advisor of the SPIE Student Chapter.